11th World Congress on Computational Mechanics (WCCM XI)
5th European Conference on Computational Mechanics (ECCM V)
6th European Conference on Computational Fluid Dynamics (ECFD VI)
E. Oñate, J. Oliver and A. Huerta (Eds)

# APPLICATION OF ADAPTIVE DYNAMIC RELAXATION TO HIGHLY NONLINEAR GEOTECHNICAL PROBLEMS

**OMID KARDANI[1], KRISTIAN KRABBENHØFT[2] AND ANDREI V. LYAMIN[3]**

[1] Australian Research Council Center of Excellence for Geotechnical Science and Engineering, School of Engineering, University of Newcastle, University Drive, Callaghan, NSW 2287 Australia
E-mail: Omid.Kardani@uon.edu.au

[2] Australian Research Council Center of Excellence for Geotechnical Science and Engineering, School of Engineering, University of Newcastle, University Drive, Callaghan, NSW 2287 Australia
E-mail: Kristian.Krabbenhoft@newcastle.edu.au

[3] Australian Research Council Center of Excellence for Geotechnical Science and Engineering, School of Engineering, University of Newcastle, University Drive, Callaghan, NSW 2287 Australia
E-mail: Andrei.Lyamin@newcastle.edu.au

**Key Words:** *Dynamic Relaxation, Nonlinear Finite Element Analysis, Computational Geomechanics.*

**Abstract.** In this paper, an adaptive dynamic relaxation technique is proposed as an efficient method for large scale nonlinear geotechnical problems. Dynamic relaxation is a numerical method to solve static problems involving highly nonlinear differential equations. Extremely simple implementation and cheap computation resulting from the underlying explicit time integration scheme make this method an attractive candidate for large scale problems. However, for highly nonlinear problems it may require large number of iterations. As a remedy, an adaptive time stepping approach is proposed to deal with changes in stiffness due to nonlinearity. Moreover, the proposed algorithm is incorporated within a 2D and 3D finite element code where analytical solution of the local governing equations, as well as global expression of the strain-displacement matrix, is utilized in order to compensate the slow convergence and enhance the performance of the algorithm. The efficiency of the proposed algorithm is verified by presenting some numerical results from 2D and 3D elastoplastic analysis of bearing capacity of circular footing with von Mises plasticity model. The results show that apart from a competitive performance for a multiple load increment procedure, this approach is capable of providing a good approximation of the failure load in a single load step.

## 1 INTRODUCTION

Nonlinear static analysis has been traditionally dealt with conventional finite element method (FEM) through a robust incremental scheme using implicit time integration techniques together with an iterative method for solution of nonlinear system of equation, such as Newton-Raphson method. The advantage of the implicit scheme is that it is unconditionally stable which allows employing large time steps. However, with problem size increasing, as for large 2D and 3D problems, the assembly and solution of large scale linear systems becomes more and more prohibitive (both in storage and computational times) even on modern computers.

Dynamic relaxation (DR) is a numerical approach for highly nonlinear static mechanical analysis. The idea behind this method is to utilize the explicit dynamic algorithms in solving a static problem, based on two observations. Firstly, the solution to a static problem can be seen as the steady-state solution of a dynamic problem. Secondly, when we seek the steady-state solution, the dynamical components, including mass, damping and the time step, is of no interest [13]. In this way, to solve a static problem, a fictitious dynamical problem is fist formed, in which the dynamical components are chosen such that the convergence rate toward the steady-state is maximized. Thus, as an explicit approach is exploited, there will be no formation and solution of linear systems of equations in an incremental analysis, which results in extremely simple implementation and very cheap computations [9, 13]. Moreover, the algorithm is highly scalable and the operations involved are efficiently parallizable. These features make DR an attractive approach particularly undertaking large scale highly nonlinear analyses on modern high-performance and massively parallel computers and computing devices.

The only disadvantage of DR is that the number of DR iterations before convergence is achieved may be quite large. A remedy is to exploit an adaptive approach to update the fictitious dynamical components occasionally in order to accommodate the substantial stiffness changes due to nonlinearity. Oakley and Knight [9] proposed an adaptive dynamic relaxation (ADR) approach for nonlinear hyper-elastic structures, in which a fictitious diagonal mass matrix as well as a damping coefficient are calculated adaptively based on the current stiffness matrix.

An overview of DR is presented in [13]. The application of DR has also been studied in various areas of science and Engineering; see for example [6, 7 and 12]. Most recently, Dang and Meguid [5] studied DR for some Geotechnical engineering problems.

In this paper, the performance of an adaptive dynamic relaxation algorithm is studied in the framework of elastoplastic finite element analysis and some modifications are proposed to enhance the performance of the algorithm, including employing analytical stress integration schemes, novel global expression of strain-displacement matrix and adaptive convergence strategy for ADR. The numerical tests on 2D and 3D footing problems verify the robustness and efficiency of the proposed algorithm.

The remaining structure of the paper is as follows. The fundamental governing equations are briefly summarized in Section 2. In Section 3, after a brief introduction to the DR method, an adaptive DR method is developed for highly nonlinear finite element analysis of geotechnical problems in Section 3. The detailed solution scheme is presented along with some improved implementation aspects In Section 4 followed by presentation and discussion of numerical results in Section 5. Finally, conclusions are drawn in section 6.

## 2 GOVERNING EQUATIONS

In this section, the governing equations of incremental elastoplasticity analysis are briefly summarized where linear elastic-perfectly plastic models are emphasized.

### 2.1 Equilibrium and strain-displacement relations

When the deformations are assumed to be infinitesimal, the strain-displacement relations are given by

$$\boldsymbol{\varepsilon} = \mathbf{B}\mathbf{u}\,, \tag{1}$$

in which $\mathbf{u}$ and $\boldsymbol{\varepsilon}$ are the displacements and strains vectors, respectively and $\mathbf{B}$ is the strain-displacement matrix. The state of static equilibrium, obtained after finite element discretization, can be expressed as:

$$\mathbf{f}_{\text{int}}(\mathbf{u}) = \mathbf{f}_{\text{ext}}\,, \tag{2}$$

where $\mathbf{f}_{\text{int}}(\mathbf{u})$ are the internal forces assumed to be a function of the displacements while $\mathbf{f}_{\text{ext}}$ are constant external forces, respectively. Moreover, the internal forces may be expressed as:

$$\mathbf{f}_{\text{int}}(\mathbf{u}) = \int_{\text{V}} \mathbf{B}^T \boldsymbol{\sigma}(\mathbf{u})\text{dV}\,, \tag{3}$$

where $\boldsymbol{\sigma}(\mathbf{u})$ are the stresses and superscript $T$ denotes the transpose matrix.

### 2.2 Constitutive relations

According to classical plasticity theory, the stresses are limited by a yield function $F(\boldsymbol{\sigma})$. In this study we focus on the use of the linear elastic/ perfectly plastic von Mises model which is one of the most basic and simple plasticity models. The total strain increment is decomposed into elastic and plastic strain increment; that is

$$d\boldsymbol{\varepsilon} = d\boldsymbol{\varepsilon}^e + d\boldsymbol{\varepsilon}^p\,. \tag{4}$$

In von Mises model, the relation between stress increment and elastic strain increment are determined by Hook’s law as

$$d\boldsymbol{\sigma} = \mathbf{D}d\boldsymbol{\varepsilon}^e\,, \tag{5}$$

in which $\mathbf{D}$ is the elastic constitutive matrix. For the plastic strain increment, von Mises model involves a yield function in the following form:

$$F(\boldsymbol{\sigma}) = \frac{1}{2}\mathbf{s}^T\mathbf{s} - k^2\,, \tag{6}$$

in which $k$ is the yield stress in pure shear and $\mathbf{s}$ are the deviatoric stresses given by

$$\mathbf{s} = \boldsymbol{\sigma} - \mathbf{m}p\,, \tag{7}$$

with $p$ being the mean stresses

$$p = \frac{1}{3}\mathbf{m}^T\boldsymbol{\sigma}\,, \tag{8}$$

and $\mathbf{m} = (1,1,1,0,0,0)^T$.

Furthermore, the plastic strain increment in this model is determined according to an associated flow rule as

$$d\boldsymbol{\varepsilon}^p = d\lambda\nabla F\,, \tag{9}$$

where $\nabla$ is the gradient operator and $d\lambda \geq 0$ is a plastic multiplier which satisfies $d\lambda F(\boldsymbol{\sigma}) = 0$. According to (5) and (9), total strain increment can be expressed as

$$d\boldsymbol{\varepsilon} = \mathbf{D}^{-1}d\boldsymbol{\sigma} + d\lambda\nabla F\,, \tag{10}$$

Thus, using (1) and (10), the stresses at each integration point are determined by the following equations

$$\begin{aligned} &\mathbf{B}(\mathbf{u}-\mathbf{u}_0) = \mathbf{D}^{-1}(\boldsymbol{\sigma}-\boldsymbol{\sigma}_0) + \lambda\nabla F \\ &F(\boldsymbol{\sigma}) \leq 0, \quad \lambda F(\boldsymbol{\sigma}) = 0, \quad \lambda \geq 0\,, \end{aligned} \tag{11}$$

where subscript $0$ refers to the initial state at the beginning of the physical load step.

## 3 ADAPTIVE DYNAMIC RELATION METHOD

In this section, the basic idea behind the dynamic relaxation (DR) method is briefly presented as in [13]. In addition, an adaptive DR (ADR) method is developed based on the one suggested by Oakley and Knight 9].

### 3.1 Dynamic relaxation

Dynamic relaxation (DR) is a numerical approach for highly nonlinear static mechanical analysis. The idea behind this method is to utilize the explicit dynamic algorithms in solving a static problem, based on two observations. Firstly, the solution to a static problem can be seen as the steady-state solution of a dynamic problem. Secondly, when we seek the steady-state solution, the dynamical components, including mass, damping and the time step, is of no interest [13]. In this way, instead of solving the static problem (2), we formulate a fictitious dynamic problem whose steady-state response matches that of the original static problem. The fictitious dynamic problem is given by:

$$\mathbf{M}\ddot{\mathbf{u}} + \mathbf{C}\dot{\mathbf{u}} + \mathbf{f}_{\text{int}}(\mathbf{u}) = \mathbf{f}_{\text{ext}}\,, \tag{12}$$

where $\mathbf{M}$ and $\mathbf{C}$ are fictitious mass and damping matrices, respectively and are chosen such that convergence rate of the dynamic problem toward the steady-state solution is accelerated.
Employing a diagonal mass matrix produced by mass lumping technique and a diagonal Rayleigh mass proportional damping of the following form leads to significant computational

advantages [2, 9]:

$$\mathbf{C} = c\mathbf{M}, \qquad c \in \Re . \tag{13}$$

Other choices for mass and damping matrices have also been studied in various applications [1, 11].

After constructing the fictitious dynamic problem, it solution is obtained through an explicit time integration method. Central difference technique is an efficient choice as it is very simple to implement and also benefits from the largest stability limit among the second-order accurate integration schemes [8, 9]. Thus, after the time discretization of problem (12) and introducing the velocity vector $\mathbf{v}$, the fictitious dynamic equations for the $n^{th}$ time increment can be written as:

$$\begin{aligned} &\mathbf{M}\dot{\mathbf{v}}_n + \mathbf{C}\mathbf{v}_n + \mathbf{f}_{\text{int}}(\mathbf{u}_n) = \mathbf{f}_{\text{ext}} \\ &\mathbf{v}_n = \dot{\mathbf{u}}_n \end{aligned} . \tag{14}$$

Oakley and Knight [9] proposed to use a half-station central difference method as it possesses a smaller order of truncation error. This defines velocities in the mid-point of the time step and the temporal derivative approximations are given by:

$$\begin{aligned} \mathbf{v}_{n+1/2} &= \frac{1}{h}(\mathbf{u}_{n+1} - \mathbf{u}_n) \\ \dot{\mathbf{v}}_n &= \frac{1}{h}(\mathbf{v}_{n+1/2} - \mathbf{v}_{n-1/2}), \\ \mathbf{v}_n &= \frac{1}{2}(\mathbf{v}_{n+1/2} + \mathbf{v}_{n-1/2}) \end{aligned} \tag{15}$$

in which $h$ is a fixed time step. By substituting equations (13) and (15) into equations (14), the governing equations for advancing the velocity and displacement to the next time increment can be expressed as:

$$\begin{aligned} &\mathbf{v}_{n+1/2} = (\frac{2-ch}{2+ch})\mathbf{v}_{n-1/2} + (\frac{2h}{2+ch})\mathbf{M}^{-1}(\mathbf{f}_{\text{ext}} - \mathbf{f}_{\text{int}}(\mathbf{u}_n)) \\ &\mathbf{u}_{n+1} = \mathbf{u}_n + h\mathbf{v}_{n+1/2} \end{aligned} , \tag{16}$$

Note that applying matrix $\mathbf{M}^{-1}$ is trivial as $\mathbf{M}$ is a diagonal matrix. Moreover, using the last equation in (15), the velocities for the first time step can be calculated by

$$\mathbf{v}_{1/2} = (\frac{2-ch}{2})\mathbf{v}_0 + (\frac{h}{2})\mathbf{M}^{-1}(\mathbf{f}_{\text{ext}} - \mathbf{f}_{\text{int}}(\mathbf{u}_0)), \tag{17}$$

with $\mathbf{v}_0$ and $\mathbf{u}_0$ being the initial velocities and displacements, respectively.

### 3.2 Evaluation of integration parameters

The critical parameters for time integration equations in (16) are the diagonal fictitious mass matrix $\mathbf{M}$, fictitious damping coefficient $c$ and time step $h$. Assuming that equations (16) are given in a simple matrix-vector product form as

$$\mathbf{u}_{n+1} = \hat{\mathbf{K}}\mathbf{u}_n , \tag{18}$$

the fastest convergence rate of convergence can be shown to be obtained for the smallest possible spectral radius $\rho = \left|\hat{\mathbf{K}}\right|$ [9]. Thus, the optimum convergence conditions can be expressed as

$$\begin{aligned} &\left|\hat{\mathbf{K}}\right| \approx (\frac{2-ch}{2+ch})^{1/2} \\ &h \approx 2(\lambda_m)^{-1/2} \quad , \\ &c \approx 2(\lambda_0)^{1/2} \end{aligned} \tag{19}$$

in which $\lambda_m$ and $\lambda_0$ are, respectively, the maximum and minimum eigenvalues of matrix $\mathbf{M}^{-1}\mathbf{K}$ with $\mathbf{K} = (\mathbf{K}_{ij})_{i,\, j=1,\ldots,m}$ being the global tangent stiffness matrix. Note that the second condition in (19) concerns with the stability of the central difference scheme based on Courant-Friedrichs-Lewy condition [3]. In practice, estimations $\lambda_m$ and $\lambda_0$ are considered. Gerschgorin's theorem provides an upper-bound estimation to $\lambda_m$ as

$$\lambda_m < \max_i \sum_{j=1}^{m} \frac{\left|\mathbf{K}_{ij}\right|}{\mathbf{M}_{ii}}, \tag{20}$$

By using (20) in the second relation in (19), a relationship can be obtained between the time step and the elements of the diagonal mass matrix as

$$\mathbf{M}_{ii} \geq \frac{h^2}{4} \sum_{j=1}^{m} \left|\mathbf{K}_{ij}\right| . \tag{21}$$

Relation (21) suggests that the step size $h$ and diagonal matrix $\mathbf{M}$ are dependent, so the time step may be fixed and then the value of the elements of $\mathbf{M}$ may be calculated. Moreover, in an element-by-element manner, (21) can be expressed as

$$\mathbf{M}_{ii} \geq \frac{h^2}{4} (\sum_{e=1}^{Nel} \sum_{j=1}^{Ndof} | k_{ij}^e |) , \tag{22}$$

where $k_{ij}^e$ are the elements of the tangent stiffness matrix, $Nel$ and $Ndof$ are the number of elements and degrees of freedom, respectively. As for the fictitious damping coefficient which is calculated from the second condition in (19), Oakley and Knight [9] recommended estimation of the minimum eigenvalue $\lambda_0$ using the mass-stiffness Rayleigh quotient as

$$\lambda_0 \approx \frac{\mathbf{v}_{n-1/2}^T \mathbf{D}_n \mathbf{v}_{n-1/2}}{\mathbf{v}_{n-1/2}^T \mathbf{M} \mathbf{v}_{n-1/2}}, \tag{23}$$

in which is the diagonal estimator of the directional stiffness after step n and is given by

$$(\mathbf{D}_n)_{ii} = \frac{(\mathbf{f}_n)_i - (\mathbf{f}_{n-1})_i}{h(\mathbf{v}_{n-1/2})_i}, \tag{24}$$

with $\mathbf{f}$ being the internal forces.

### 3.4 Stability of the algorithm

For highly nonlinear problems, the stiffness conditions may undergo significant changes during the course of analysis. In order to accommodate these changes and ensure the stable convergence of the method, the integration parameters need to be updated accordingly. The damping coefficient can be computed cheaply in each ADR iterations. However, the calculation of the mass matrix through (22) is usually computationally expensive due to the required stiffness calculation. It is, therefore, desirable to update the mass matrix occasionally only when the stability of the algorithm is critically perturbed.

Park and Underwood [10] suggested stability criteria based on the perturbed apparent frequency error estimators $e_i$ which is given by

$$e_i = \frac{h^2}{4} \frac{|(\dot{\mathbf{v}}_n)_i - (\dot{\mathbf{v}}_{n-1})_i|}{|(\mathbf{u}_n)_i - (\mathbf{u}_{n-1})_i|}. \tag{25}$$

If the values of the error estimators are larger than one, the ADR algorithm with the current fictitious mass matrix $\mathbf{M}$ is considered to be unstable and $\mathbf{M}$ needs to be updated in order to stabilize the algorithm.

## 4 SOLUTION SCHEME

Based on what was discussed so far, the global discrete governing equations can be given as

$$\mathbf{v}_{n+1/2} = \left(\frac{2-ch}{2+ch}\right)\mathbf{v}_{n-1/2} + \left(\frac{2h}{2+ch}\right)\mathbf{M}^{-1}\left(\mathbf{f}_{\text{ext}} - \int_V \mathbf{B}^T \boldsymbol{\sigma}_n \mathrm{dV}\right) \tag{26}$$

$$\mathbf{u}_{n+1} = \mathbf{u}_n + h\mathbf{v}_{n+1/2} \tag{27}$$

$$\begin{aligned} &\mathbf{B}(\mathbf{u}_{n+1} - \mathbf{u}_0) = \mathbf{D}^{-1}(\boldsymbol{\sigma}_{n+1} - \boldsymbol{\sigma}_0) + \lambda \nabla F(\boldsymbol{\sigma}_{n+1}) \\ &F(\boldsymbol{\sigma}_{n+1}) \le 0, \quad \lambda F(\boldsymbol{\sigma}_{n+1}) = 0, \quad \lambda \ge 0 \end{aligned} \tag{28}$$

### 4.1 Global strain-displacement matrix

A clever idea to improve the computational efficiency of the algorithm is to assemble a sparse global strain-displacement matrix once in the beginning of the analysis and then used throughout the process. In this way, $\mathbf{B}$ is actually consists of the element strain-displacement matrices which are assembled in a sparse matrix format. Note that exploiting a global strain-displacement matrix is possible in finite element analysis subject to material nonlinearity since $\mathbf{B}$ is independent of the integration parameter in (3).

Thus, the calculations of the internal forces operations may be performed in an efficient sparse matrix-vector product manner as

$$\mathbf{f}_{\text{int}}(\mathbf{u}) = \mathbf{B}^T . \int_{\text{V}} \boldsymbol{\sigma}(\mathbf{u}) \text{dV}, \quad (29)$$

This is an attractive feature in terms of computational efficiency of large scale analysis and is of particular interest for parallel implementation of the algorithm on massively parallel machines.

### 4.2 Convergence criteria

Another important aspect in an elaborate implementation of the algorithm is the choice of the convergence criteria for the ADR iterations. There are three convergence criteria traditionally employed for nonlinear finite element analysis, including the unbalanced force-based, displacement-based and internal energy-based criteria.

We propose a hybrid convergence criterion which seems to lead to a more consistent and stable analysis throughout different load increments. It consists of two measures for the quality of the updates in each ADR iteration. The first one is a criterion based on energy considerations proposed in [9]:

$$\theta_n^1 = \left| \frac{\mathbf{v}_{n-1/2}^T \mathbf{M} \mathbf{v}_{n-1/2}}{\mathbf{u}_n^T \mathbf{f}_n} \right| < \varepsilon_1, \quad (30)$$

in which $\varepsilon_1 > 0$ is a stopping tolerance. We observed that this convergence criteria may lead to inconsistent behaviour of the algorithm. In other words, the large values of $\varepsilon_1$ lead to lack of accuracy while smaller values increase the time of analysis, usually without any significant improvement to the accuracy. Therefore, we introduce a second criterion to our proposed convergence criteria in which the norms of the inertial terms, i.e. the velocity and acceleration, are considered as follows:

$$\theta_n^2 = \max(\|\mathbf{v}_n\|_\infty, \|\dot{\mathbf{v}}_n\|_\infty) < \varepsilon_2, \quad (31)$$

in which $\|.\|_\infty$ denotes the infinity norm and $\varepsilon_2 > 0$ is a stopping tolerance. Then, the second criteria is satisfied when the number of consecutive iterations for which $\theta_n^2 < \varepsilon_2$ is more than a maximum allowed number $\eta$. In this way, in addition to considering the static equilibrium, we ensure that the inertial part of the fictitious dynamic problem vanishes. This hybrid driteria allows for relatively larger values of $\varepsilon_1 > 0$ and $\varepsilon_2 > 0$.

### 4.3 Solution Algorithm

The incremental nonlinear finite element analysis scheme using ADR algorithm is summarized in the following algorithm:

1. Input finite element mesh information
2. Assemble global matrix $\mathbf{B}$
3. Loop 1: over load increments
    - 3.1. Compute current load increment $\mathbf{f}_{\text{ext}}$
    - 3.2. Compute $\mathbf{M}$ from (22)
    - *Initialization:*
    - 3.3. Set $\mathbf{u}_0 = 0, \mathbf{v}_0 = 0, \mathbf{f}_{\text{int}}(\mathbf{u}_0) = 0$
    - 3.4. Compute $c$ by (23)
    - 3.5. Compute $\mathbf{v}_{1/2}$ by (17)
    - 3.6. Compute $\mathbf{u}_1$ from (27)
    - 3.7. Loop 2: over ADR iterations
        - 3.7.1. Set $i = 1$
        - 3.7.2. Check (25) and if unstable update $\mathbf{M}$ from (22)
        - 3.7.3. Compute global $\boldsymbol{\sigma}_i$ by (28)
        - 3.7.4. Compute $\mathbf{f}_{\text{int}}(\mathbf{u}_i)$ by (29)
        - 3.7.5. Compute $c$ by (23)
        - 3.7.6. Compute $\mathbf{v}_{i+1/2}$ by (26)
        - 3.7.7. Compute $\mathbf{u}_{i+1}$ from (27)
        - 3.7.8. Check convergence from (30) and (31) and stop if converged.
    - 3.8. End loop 2
4. End loop 1 and the analysis

## 5 NUMERICAL EXAMPLE

In this section, the numerical results of the dynamic relaxation algorithm with the proposed implementation scheme are presented for a rough-based circular footing problem. The material properties are given in Table 1. A schematic of the problem geometry as well as a typical 3D finite element mesh is illustrated in Figure 1. Note that due to the symmetry of the geometry, only a quarter of the footing is modelled.

**Table 1:** Material properties

| Material | Cohesion (kPa) | Friction angle | Dilation angle | Poisson's ratio | Young's modulus (kPa) | Unit weight ($kN/m^3$) |
|---|---|---|---|---|---|---|
| von Mises | 1.0 | 0.0 | 0.0 | 0.3 | 1000 | 0.0 |

The performance of the proposed adaptive dynamic relaxation algorithm is studied for four meshes with increasing number of elements. For all of them, quadratic 10-noded tetrahedral elements with reduced integration (4 Gauss points) are utilized [14]. Also, the tolerance values for the proposed hybrid convergence criteria are set as $\varepsilon_1 = 1.e-3,\ \varepsilon_1 = 1.e-5,\ \eta = 100$ for all numerical tests. As mentioned before, employing a hybrid convergence criteria allows the use of relatively large stopping tolerances. Table 2 summarizes the properties of the examined meshes.

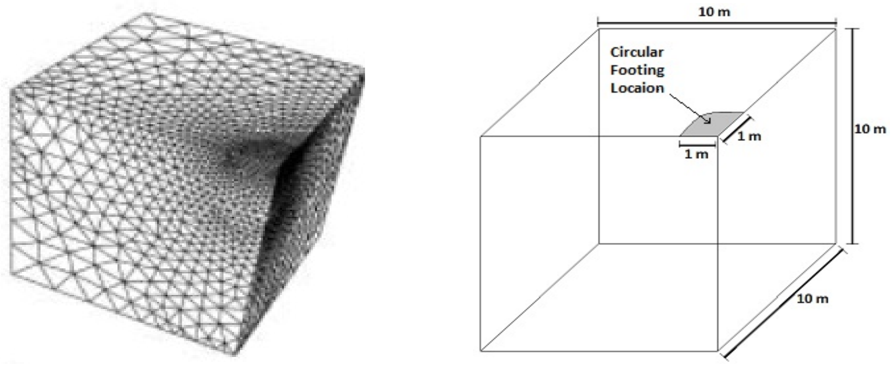


**Figure 1:** Typical mesh and geometry of the circular footing problem

**Table 2:** Mesh information

| Mesh | Nodes No. | Elements No. |
|---|---|---|
| **1** | 1,261 | 720 |
| **2** | 8,825 | 5,760 |
| **3** | 28,453 | 19,440 |
| **4** | 65,905 | 46,080 |

The load-displacement curves related to an analysis using 20 load increments are illustrated in Figure 2. For the sake of comparison, the exact theoretical value for the rough-based circular footing on Tresca soil (6.05 kPa) proposed by Cox et al. [4] is also presented in Figure 2.

It can be seen in Figure 2 that a more refined mesh improves the accuracy of the failure load approximate. This verifies the robustness of the proposed solution scheme. Moreover, the estimated failure load is in a good agreement with the theoretical failure load. In fact, the failure loads captured by examined meshes vary from 1.34 to 1.015 times the theoretical failure load depending on the coarseness of the meshes. This verifies the correctness of the proposed algorithm.

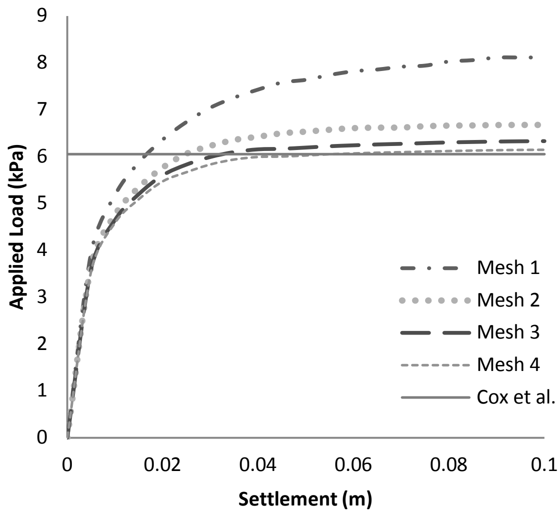


**Figure 2:** Applied load vs. displacement for four sample meshes

In order to investigate the computational efficiency of the proposed solution scheme more precisely, numerical results of performing the analysis with different settings of the meshes and the number of load increments are given in Table 3. These results contain the total number of ADR iterations required for convergence, the total execution time as well as the Failure Load Error percentage which is calculated as

$$\frac{\text{Estimated Failure Load - 6.05}}{6.05}\times 100 \; .$$

The analysis is performed by introducing prescribed displacements under the circular footing.

**Table 3:** Numerical results from incremental finite element analysis for four meshes

| Problem | No. of Load Increments | Failure Load Error (%) | Total ADR Iterations | Total Time (s) |
|---|---|---|---|---|
| **1** | 20 | 34.1 | 69,807 | 74.97 |
| | 10 | 31.9 | 22,956 | 25.22 |
| | 1 | 31.4 | 1,138 | 1.23 |
| **2** | 20 | 10.2 | 198,953 | 1854.55 |
| | 10 | 9.5 | 84,479 | 787.72 |
| | 1 | 9.2 | 2,722 | 25.46 |
| **3** | 20 | 4.4 | 560,433 | 17857.30 |
| | 10 | 3.6 | 228,980 | 7362.61 |
| | 1 | 3.1 | 7,258 | 230.16 |
| **4** | 20 | 1.9 | 753,731 | 57609.79 |
| | 10 | 1.4 | 383,218 | 27290.03 |
| | 1 | 1 | 16,483 | 1135.50 |

According to Table 3, the computation times of the analysis are fairly promising. Indeed, exploiting a global strain-displacement matrix as well as the return mapping procedure for stress integration minimizes the time required for each ADR iteration. The errors in the estimated failure load decrease as the mesh becomes finer. This verifies the robustness of the algorithm. Moreover, the accuracy of the estimated failure loads for the finest mesh, Mesh 4, is very promising. Another interesting finding in Table3 is that a single load increment can approximate the final failure load with a good accuracy. In fact, it gives rise to an upper bound approximation for the exact failure load. Moreover, such a good approximation is achievable with minimal computations of a single load.

## 6 CONCLUSION

In this paper, the performance of an adaptive dynamic relaxation scheme is studied for highly nonlinear geotechnical problems. In addition to efficient configuration of ADR algorithm, some other techniques were proposed to improve the computational efficiency of the analysis, including assembly and employing a sparse global strain-displacement matrix which reduces the computation of strains and internal forces to sparse matrix-vector products, undertaking a return mapping procedure for calculating plastic stresses and implementing hybrid convergence criteria for ADR iterations. Our numerical results verify the correctness and robustness of the proposed algorithm with an emphasis on the computational efficiency. Finally, using the proposed ADR algorithm, a good approximation to the failure load is achieved in a singly load increment. For future research, we are investigating the parallel implementation of the proposed algorithm on Graphic Processing Unit (GPU) in order to improve the computation times for large scale nonlinear finite element analysis.

## REFERENCES


[1] Alamatian, J. A new formulation for fictitious mass of the dynamic relaxation method with kinetic damping. *Comput. Struct.* (2012) **90**:42-54.

[2] Belytschko, T. and Mullen, R. Explicit integration of structural problems, in: Bergan, P. et al., eds., *Finite Elements in Nonlinear Solid and Structural Mechanics*, Trondheim, Norway (1977).

[3] Courant, R., Friedrichs, K. and Lewy, H. On the partial difference equations of mathematical physics. IBM J. (1967) 215-234.

[4] Cox, A.D., Eason, G. and Hopkins, H.G. Axially symmetric plastic deformation in soils. *Phil. Trans. R. Soc. London, Ser. A* (1961) **254**:1-45.

[5] Dang, H.K. and Meguid, M.A. Evaluating the performance of an explicit dynamic relaxation technique in analysing nonlinear geotechnical engineering problems. *Comput. Geotech.* (2010) **37**:125-131.

[6] Joldes, G.R., Wittek, A. and Miller, K. An adaptive dynamic relaxation method for solving nonlinear finite element problems. *Int. J. Num. Meth. Biomed. Engng* (2011) **27**:173–185.

[7] Kashiwa, M. and Onoda, J. Wrinkling analysis using improved dynamic relaxation method. *American Inst. Aeron. Astron. J.* (2009) **47**. DOI: 10.2514/1.34031.

[8] Krieg, R. Unconditional stability in numerical time integration methods. *ASME J. Appl. Mech.* (1973) **40**:417-421.

[9] Oakley, D.R. and Knight, N.F. Adaptive dynamic relaxation algorithm for non-linear hyper-elastic structures Part I: Formulation. *Comput. Meth. Appl. Mech. Engng* (1995) **126**:67–89.

[10] Park, K. and Underwood, P. A variable-step central difference method for structural dynamics analysis Part 1: Theoretical aspects. *Comput. Meth. Appl. Mech. Engng* (1980) **22**:241-258.

[11] Rezaiee-pajand, M. and Alamatian, J. The dynamic relaxation method using new formulation for fictitious mass and damping. *Struct. Engng. Mech.* (2010) **34**:109-133.

[12] Salehi and M., Aghaei, H. Dynamic relaxation large deflection analysis of non-axisymmetric circular viscoelastic plates. *Comput. Struct.* (2005) **83**:1878–1890.

[13] Underwood, P., Dynamic relaxation, in: Belytschko, T. and Hughes, T.J.R., eds., *Computational Methods for Transient Dynamic Analysis*. North Holland, Amsterdam, (1983), 246-265.

[14] Zienkiewicz, O.C. and Taylor, R.L. *The finite element method*. *Its basis and fundamentals*. 6th ed., Elsevier, (2005).